Table 1
Primers used for quantification of mRNA levels

Accession no.	Definition	Forward primer	Reverse primer
U48247	Enigma	ttcgtctccaccaaacactg	tccctctgctagctcctgag
Z46614	Caveolin1	gcatcctctctttcctgcac	tggaatagacacggctgatg
U44948	SmLIM	taatgtggatggccttaccg	ggatgggcaggagagtgtag
AF000942	Id3a	cctcgaccttcaagtggttc	acgttcagatgagcctggtc
M17701	Glyceraldehyde-3-phosphate-dehydrogenase	cttccgtgttcctaccc	acctggtcctcagtgtagcc
M83107	SM22	tgagcaagttggtgaacagc	attgagccacctgttccatc
X06801	αSMactin	gctctggtgtgtgacaatgg	aaccatcactccctggtgtc
U50044	von Willebrand factor	agcgggtgaaatacctagcc	gcagtcagttggcctctacc

5% CO2. VSMC at 6–10 passages were used in the experiments. Cells were seeded in 10-cm-culture dishes to grow to confluence. Then, the medium was replaced with phenol red-free RPMI1640 (Sigma) containing 100 nM E2 (Sigma) or vehicle (0.1% ethanol). Twenty-four hours later, cells were washed with phosphate-buffered saline twice and homogenized immediately in Isogen reagent (Nippon Gene, Osaka, Japan).

Northern blot analysis

Twenty micrograms of total RNA from cultured VSMC were fractionated on 1.3% formaldehyde-agarose gel and transferred to nylon filters (Hybond-N, Amersham Life Science Inc.). The filters were hybridized with random-primed ^{32}P-labeled rat cDNA probes and autoradiographed. To synthesize cDNA probes, reverse transcription-PCR was performed using RNA prepared from VSMC with primers specific for each gene. The primers were synthesized according to the published rat cDNA sequences as follows: (forward/reverse)

Enigma: 5′-gccttctcagcagtcagctt-3′/5′-ttcttctggatgccaggact-3′
Caveolin-1: 5′-cgtagactccgagggacatc-3′/5′-gctcttgatgcacggtacaa-3′
Smooth muscle LIM protein (SmLIM): 5′-gaagaggtgcagtgtgatgg-3′/5′-tctggagcacttctcagcac-3′
Inhibitor of DNA binding 3a (Id3a): 5′-ggaacgtagcctagccattg-3′/5′-ttcagatgagcctggtctagc-3′.

Amplified PCR products were subcloned into a plasmid vector, pCR2.1 vector, and sequenced. An oligonucleotide probe complementary to 18S rRNA was used to confirm the equal loading of RNA. (Watanabe et al., 2001) The filters were autoradiographed, and the bands were scanned and the density was determined with Scion software (Scion image ver 3.0, Scion Corp.).

Statistical analysis

The mRNA levels calculated in real-time PCR were analyzed using one-way ANOVA. When a statistically significant effect was found, Newman-Keul's test was performed to isolate the difference between the groups. A value of $P < 0.05$ was considered significant. All data in the text and figures are expressed as mean ± SE.

Results

Screening for genes expressed differently between OVX + V and OVX + E by high-density oligonucleotide array

We first performed a global expression analysis of approximately 7000 genes using a high-density oligonucleotide microarray to identify estrogen-regulated genes in the rat aorta. Around 2000 genes were considered to be present in the aorta according to our criteria. As shown in Table 2, the expression of control GAPDH was comparable among the groups, suggesting that the microarray assay worked well. The expression of SM22 was high, whereas that of von Willebrand factor and endothelial nitric oxide synthase was below the detection level. These findings indicate that the samples were mainly derived from the medial layer of the aorta. In this screening, we identified approximately 200 genes, the expression levels of which were different between the OVX + E group and OVX + V group. We, first, checked the genes reported to be regulated by estrogen in the aorta, such as angiotensin II type 1 receptor (Nickenig et al., 1998), angiotensin converting enzyme (Gallagher et al., 1999), and c-fos (Akishita et al., 1996), and in reproductive tissues, such as progesterone receptor (May et al., 1989), c-myc (Weisz and Bresciani, 1988), and glucose-6-phosphate dehydrogenase (Korach et al., 1985). Consistent with the previous data, the intensity of angiotensin converting enzyme in OVX + E was down-regulated to nearly 50% compared to that in OVX + V. However, AT1 receptor, c-myc and progesterone receptor were not detected in aorta by high-density oligonucleotide microarray analysis probably because of the low sensitivity to these genes. Also, in sham-operated rats, the intensity of c-fos gene was at much higher level compared to that in OVX + V. The reason for a tremendous increase of c-fos expression might result from unknown stresses, because the intensity of several immediate-early genes was also increased in sham-operated rats (data not shown). The explanations for these results were that the sensitivity of probes for several genes was under the threshold, and/or that the reproducibility was not high due to small number of samples in each group (n = 2). Then, among the 200 genes, we focused on up to 20 candidate genes, which were reported to be expressed in the vasculature.

Table 2
Expression of marker genes and previously reported estrogen-regulated genes in aorta

Accession No.	Definition	Sham (Intensity)	OVX+V (Intensity)	OVX+E (Intensity)
M17701	Glyceraldehyde-3-phosphate-dehydrogenase	1278.5	1232.6	1246.0
M83107	SM22	4350.8	4487.8	4631.9
U50044	von Willebrand factor	8.7	-54.8	-19.8
AF110508	endothelial nitric oxide synthase	48.4	48.1	45.3
M90065	angiotensin II receptor	-7.5	5.1	4.2
U03734	angiotensin converting enzyme	216.6	239.9	148.3
X06769	c-fos	1800.1	307.7	231.8
S64044	progesterone receptor	61.3	31.7	39.8
X07467	glucose-6-phosphate dehydrogenase	474.0	332.1	454.2
Y00396	c-myc	44.4	36.3	33.3

Table 3
Genes with altered expression level in aorta according to DNA microarray technique

Accession no.	Definition	Sham (intensity)	OVX+V (intensity)	OVX+E (intensity)	OVX+E/OVX+V
U48247	Enigma	288.3	128.6	455.5	3.5
Z46614	Caveolin-1	674.3	329.1	694.4	2.1
U44948	SmLIM	1266.9	1260.7	2054.9	1.6
AF000942	Id3a	201.7	224.6	318.3	1.4

Confirmation of estrogen-regulated genes in aorta by real-time PCR

Next, we performed real-time PCR to examine the expression of the candidate genes obtained from the microarray. In real-time PCR, we used primers that amplified sequences different from the microarray. Subsequently, four genes, caveolin1, enigma, SmLIM and Id3a, were identified as being upregulated in the OVX + E group (Table 3 and Fig. 1). On the other hand, we could not identify any genes down-regulated in the OVX + E group in this study, so far. To exclude the possibility of the contamination with other cell types in total RNA samples we used, we compared the intensity of these four genes and markers for endothelium or VSMC in the samples between with or without endothelium obtained from intact 8-week-old male rats (n = 12) (Fig. 2). Semi-quantitative analysis by real-time PCR showed that these four genes and markers of VSMC were expressed comparably between samples with or without endothelium. In contrast, the expression of an endothelial marker, von Willebrand factor, was scanty in endothelium-denuded samples. Specific markers for adventitial fibroblasts have not been identified (Sartore et al., 2001). Therefore, we cannot exclude the contamination with adventitial fibroblasts, although the adventitial layer is very small in amount compared with smooth muscle layers.

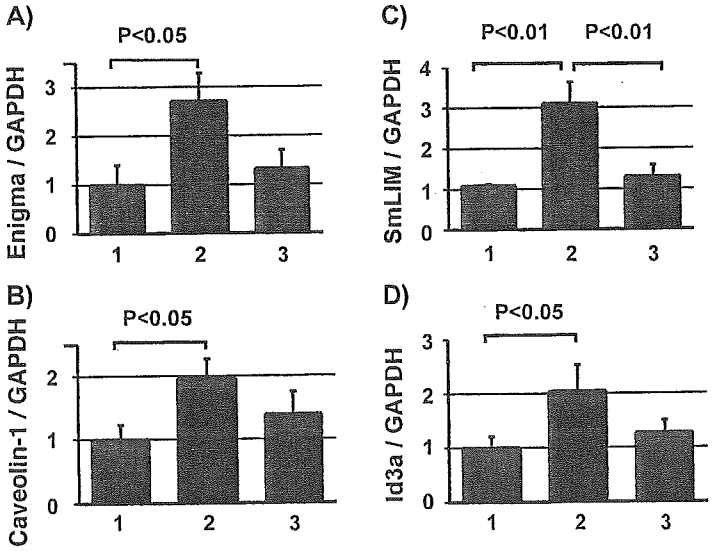

Fig. 1. Real-time PCR comparing expression of enigma, caveolin-1, SmLIM and Id3a in aortic tissue. Total RNA was obtained from the aorta of OVX + V (lane 1, n = 5), OVX + E (lane 2, n = 5), and Sham (lane 3, n = 4) groups, and reverse-transcribed into cDNA. Then, 50 ng cDNA was amplified using primers specific for each gene sequence using real-time PCR method. The starting quantities were calculated and expressed as the ratio of each gene to GAPDH. Values are shown as mean ± SE.

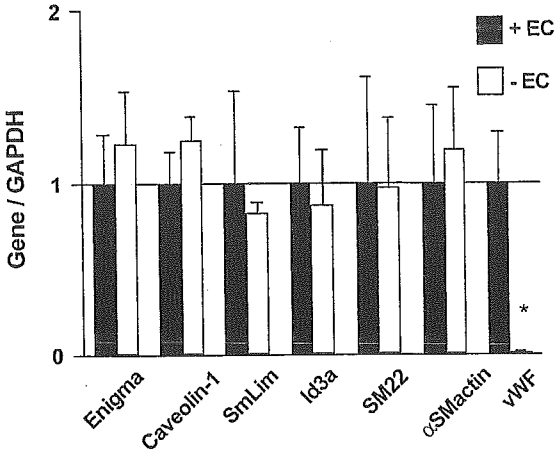

Fig. 2. The expression levels in the identified genes and maker genes in the samples with or without endothelium (EC). The aortic tissues were obtained from intact 8-week male rats, and were divided into two groups; with EC (n=6) and without EC (n=6). Real-time PCR was performed as described above, and the starting quantities were calculated and expressed as the ratio of each gene to GAPDH. Values are shown as the ratio of the samples with EC to that without EC and as mean ± SE. *, $p<0.01$ vs + EC. EC; endothelium, vWF; von Willebrand factor.

E2-induced expression of genes in cultured VSMC

In order to investigate whether E2 could directly regulate the expression of these four genes, we examined their mRNA levels in cultured VSMC by Northern blot analysis. As shown in Fig. 3, treatment with E2 for 24 hours increased the mRNA levels of caveolin1, enigma, SmLIM and Id3a mRNA.

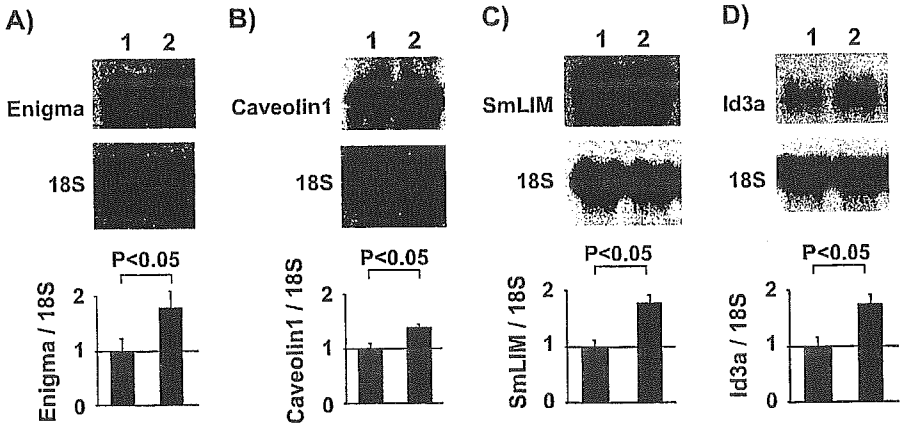

Fig. 3. Northern blot analysis of enigma, caveolin-1, SmLIM1 and Id3a in cultured VSMC. VSMC were treated with vehicle (lane 1) or 100 nmol/L E2 (lane 2) for 24 hours. Total RNA was extracted from VSMC, and 20 μg total RNA per lane was used for Northern blot analysis. The membrane was hybridized to a 32P-labeled cDNA probe specific for each gene and to an 18S probe to assess loading differences. In different sets of experiments, mRNA levels of indicated genes were measured by densitometry and expressed as the ratio of genes to 18S. Similar results were obtained in three independent experiments.

Discussion

In the present study, we screened for genes that responded to estrogen stimulation in VSMC. We newly identified genes upregulated by estrogen; enigma, SmLIM, caveolin and Id3a, in VSMC.

Caveolin-1 is one subtype of caveolins, which are principal coat proteins of caveolae (Severs, 1988). Caveolae, the flask-shaped vesicular invaginations of the plasma membrane, are present in many cell types including VSMC (Drab et al., 2001). Caveolae function in signal transduction (Okamoto et al., 1998) as well as in endocytosis and transcytosis in vesicular transport (Schnitzer et al., 1995). Mice lacking the caveolin-1 gene show impaired endothelium-dependent relaxation, contractility and maintenance of myogenic tone of the aorta through nitric oxide and Ca^{2+} signaling (Drab et al., 2001). Several studies have reported the role of caveolin-1 in estrogen-mediated signaling in vascular cells. In vascular endothelium, nitric oxide synthase is activated rapidly by estrogen following binding with ERα in caveolae (Chambliss et al., 2000). In VSMC, estrogen stimulated the binding of ERα with caveolin-1 and augmented the production of caveolin-1 through a transcriptional mechanism (Razandi et al., 2002). Consistent with this report, we showed that estrogen upregulated mRNA expression of caveolin-1 in the aorta, as well as in cultured VSMC. Taken together, estrogen-mediated upregulation of cavelin-1 might be related to the improvement of vascular function.

Two LIM protein genes and one member of the Id gene family were also identified as estrogen-regulated genes in the aorta in the present study. LIM proteins are a protein family containing the LIM motif, a double-zinc-finger structure. The LIM motif has been proposed to participate in protein-protein interactions (Dawid et al., 1995; Sanchez-Garcia and Rabbitts, 1994), and to be critical in cellular determination and differentiation (Arber and Caroni, 1996; Schmeichel and Beckerle, 1994). SmLIM, one of the LIM proteins, is expressed principally in VSMC of adult animals and is induced in VSMC during development, preceding the appearance of the smooth muscle myosin heavy chain, a sensitive indicator of VSMC differentiation (Jain et al., 1998). Moreover, SmLIM localizes in the nucleus and in actin-based filaments in the cytosol. Therefore, SmLIM is thought to coordinate cytoskeletal function and subsequently regulate cellular proliferation and differentiation (Jain et al., 1998). Another LIM protein, enigma, belongs to the PDZ-LIM protein, and is expressed abundantly in skeletal muscle as well as in non-muscle cells (Durick et al., 1998; Guy et al., 1999). The PDZ domain of enigma binds to a skeletal muscle target, the actin-binding protein, tropomyosin, suggesting that enigma is an adapter protein that directs the LIM-binding protein to actin filaments of muscle cells (Guy et al., 1999). The inhibitor of DNA binding (Id), a class of helix-loop-helix transcription factors, is known to regulate growth in many cells including VSMC (Matsumura et al., 2001; Norton et al., 1998; Olson, 1990). There are four known Id genes, Id1 to Id4. Id3a is produced by alternative splicing of the Id3 gene, resulting in inclusion of a 115-bp "coding intron", which encodes a unique 29-amino-acid carboxyl terminus of the Id3a protein (Matsumura et al., 2001). It is reported that Id3a is associated with apoptotic activity in VSMC (Matsumura et al., 2001). In contrast, another group showed that Id3 mediated angiotensin II-induced cell growth (Mueller et al., 2002); therefore, the precise role of Id3 and its splice variant, Id3a, in the vasculature, has not been determined.

There are no reports with respect to the regulation of these three genes by estrogen, not only in the vasculature but also in other organs, so our findings might imply a new understanding of mechanisms of the effects of estrogen in the vascular wall. Because SmLIM and Id3a may be associated with cell growth and differentiation, these genes might mediate the effects of estrogen on VSMC growth and differentiation. Enigma is considered to be an adaptor protein, which can connect some kinases or

phosphatases with the membrane (Cuppen et al., 1998; Kuroda et al., 1996). Therefore, it can be hypothesized that enigma would mediate the effects of estrogen such as growth inhibition in VSMC through the binding with some phosphatases such as SHP-1 or MKP-1 which could be induced by estrogen (Takeda-Matsubara et al., 2002).

Downstream of the estrogen-ER signaling pathway has not been clarified in the vasculature as much as in reproductive organs. Estrogen augmented the promoter activity of caveolin-1, which did not contain any palindrome estrogen responsive elements in the 3 kb promoter region (Razandi et al., 2002). The sequences of the promoter region of SmLIM, enigma, and Id3 genes have not been reported. Analysis of the promoter of these genes may provide some hints to understand the downstream signals of ER in the vasculature. Also, in this study, we could not check all of the genes expressed differentially between the OVX + E group and OVX + V group obtained from the high-oligonucleotide microarray analysis. Thus, further study should be done to identify other estrogen-regulated genes that might play more important roles in the vasculature.

Acknowledgements

This work was supported by a Grant-in-Aid from the Ministry of Education, Science, Sports and Culture of Japan (13557062) and a Grant-in-Aid for Science Research from the Ministry of Health, Labor and Welfare of Japan (H13-Choju-016).

References

Akishita, M., Ouchi, Y., Miyoshi, H., Orimo, A., Kozaki, K., Eto, M., Ishikawa, M., Kim, S., Toba, K., Orimo, H., 1996. Estrogen inhibits endothelin-1 production and c-fos gene expression in rat aorta. Atherosclerosis 125 (1), 27–38.

Arber, S., Caroni, P., 1996. Specificity of single LIM motifs in targeting and LIM/LIM interactions in situ. Genes Dev. 10 (3), 289–300.

Bell, D.R., Rensberger, H.J., Koritnik, D.R., Koshy, A., 1995. Estrogen pretreatment directly potentiates endothelium-dependent vasorelaxation of porcine coronary arteries. Am. J. Physiol. 268 (1 Pt 2), H377–H383.

Brown, A.M., Jeltsch, J.M., Roberts, M., Chambon, P., 1984. Activation of pS2 gene transcription is a primary response to estrogen in the human breast cancer cell line MCF-7. Proc. Natl. Acad. Sci. USA 81 (20), 6344–6348.

Chambliss, K.L., Yuhanna, I.S., Mineo, C., Liu, P., German, Z., Sherman, T.S., Mendelsohn, M.E., Anderson, R.G., Shaul, P.W., 2000. Estrogen receptor alpha and endothelial nitric oxide synthase are organized into a functional signaling module in caveolae. Circ. Res. 87 (11), E44–E52.

Colditz, G.A., Willett, W.C., Stampfer, M.J., Rosner, B., Speizer, F.E., Hennekens, C.H., 1987. Menopause and the risk of coronary heart disease in women. N. Engl. J. Med. 316 (18), 1105–1110.

Cuppen, E., Gerrits, H., Pepers, B., Wieringa, B., Hendriks, W., 1998. PDZ motifs in PTP-BL and RIL bind to internal protein segments in the LIM domain protein RIL. Mol. Biol. Cell 9 (3), 671–683.

Dawid, I.B., Toyama, R., Taira, M., 1995. LIM domain proteins. C. R. Acad. Sci. III 318 (3), 295–306.

Drab, M., Verkade, P., Elger, M., Kasper, M., Lohn, M., Lauterbach, B., Menne, J., Lindschau, C., Mende, F., Luft, F.C., Schedl, A., Haller, H., Kurzchalia, T.V., 2001. Loss of caveolae, vascular dysfunction, and pulmonary defects in caveolin-1 gene-disrupted mice. Science 293 (5539), 2449–2452.

Durick, K., Gill, G.N., Taylor, S.S., 1998. Shc and Enigma are both required for mitogenic signaling by Ret/ptc2. Mol. Cell Biol. 18 (4), 2298–2308.

Gallagher, P.E., Li, P., Lenhart, J.R., Chappell, M.C., Brosnihan, K.B., 1999. Estrogen regulation of angiotensin-converting enzyme mRNA. Hypertension 33 (1 Pt. 2), 323–328.

Guy, P.M., Kenny, D.A., Gill, G.N., 1999. The PDZ domain of the LIM protein enigma binds to beta-tropomyosin. Mol. Biol. Cell. 10 (6), 1973–1984.

Hodges, Y.K., Tung, L., Yan, X.D., Graham, J.D., Horwitz, K.B., Horwitz, L.D., 2000. Estrogen receptors alpha and beta: prevalence of estrogen receptor beta mRNA in human vascular smooth muscle and transcriptional effects. Circulation 101 (15), 1792–1798.

Hulley, S., Grady, D., Bush, T., Furberg, C., Herrington, D., Riggs, B., Vittinghoff, E., 1998. Randomized trial of estrogen plus progestin for secondary prevention of coronary heart disease in postmenopausal women. Heart and Estrogen/progestin Replacement Study (HERS) Research Group. Jama 280 (7), 605–613.

Inoue, S., Orimo, A., Hosoi, T., Kondo, S., Toyoshima, H., Kondo, T., Ikegami, A., Ouchi, Y., Orimo, H., Muramatsu, M., 1993. Genomic binding-site cloning reveals an estrogen-responsive gene that encodes a RING finger protein. Proc. Natl. Acad. Sci. USA 90 (23), 11117–11121.

Ishii, M., Hashimoto, S., Tsutsumi, S., Wada, Y., Matsushima, K., Kodama, T., Aburatani, H., 2000. Direct comparison of GeneChip and SAGE on the quantitative accuracy in transcript profiling analysis. Genomics 68 (2), 136–143.

Jain, M.K., Kashiki, S., Hsieh, C.M., Layne, M.D., Yet, S.F., Sibinga, N.E., Chin, M.T., Feinberg, M.W., Woo, I., Maas, R.L., Haber, E., Lee, M.E., 1998. Embryonic expression suggests an important role for CRP2/SmLIM in the developing cardiovascular system. Circ. Res. 83 (10), 980–985.

Kannel, W.B., Hjortland, M.C., McNamara, P.M., Gordon, T., 1976. Menopause and risk of cardiovascular disease: the Framingham study. Ann. Intern. Med. 85 (4), 447–452.

Karas, R.H., Patterson, B.L., Mendelsohn, M.E., 1994. Human vascular smooth muscle cells contain functional estrogen receptor. Circulation 89 (5), 1943–1950.

Korach, K.S., Fox-Davies, C., Quarmby, V.E., Swaisgood, M.H., 1985. Diethylstilbestrol metabolites and analogs. Biochemical probes for differential stimulation of uterine estrogen responses. J. Biol. Chem. 260 (29), 15420–15426.

Kuroda, S., Tokunaga, C., Kiyohara, Y., Higuchi, O., Konishi, H., Mizuno, K., Gill, G.N., Kikkawa, U., 1996. Protein-protein interaction of zinc finger LIM domains with protein kinase C. J. Biol. Chem. 271 (49), 31029–31032.

Matsumura, M.E., Li, F., Berthoux, L., Wei, B., Lobe, D.R., Jeon, C., Hammarskjold, M.L., McNamara, C.A., 2001. Vascular injury induces posttranscriptional regulation of the Id3 gene: cloning of a novel Id3 isoform expressed during vascular lesion formation in rat and human atherosclerosis. Arterioscler. Thromb. Vasc. Biol. 21 (5), 752–758.

May, F.E., Johnson, M.D., Wiseman, L.R., Wakeling, A.E., Kastner, P., Westley, B.R., 1989. Regulation of progesterone receptor mRNA by oestradiol and antioestrogens in breast cancer cell lines. J. Steroid. Biochem. 33 (6), 1035–1041.

Mueller, C., Baudler, S., Welzel, H., Bohm, M., Nickenig, G., 2002. Identification of a novel redox-sensitive gene, Id3, which mediates angiotensin II-induced cell growth. Circulation 105 (20), 2423–2428.

Nickenig, G., Baumer, A.T., Grohe, C., Kahlert, S., Strehlow, K., Rosenkranz, S., Stablein, A., Beckers, F., Smits, J.F., Daemen, M.J., Vetter, H., Bohm, M., 1998. Estrogen modulates AT1 receptor gene expression in vitro and in vivo. Circulation 97 (22), 2197–2201.

Norton, J.D., Deed, R.W., Craggs, G., Sablitzky, F., 1998. Id helix-loop-helix proteins in cell growth and differentiation. Trends Cell Biol. 8 (2), 58–65.

Okamoto, T., Schlegel, A., Scherer, P.E., Lisanti, M.P., 1998. Caveolins, a family of scaffolding proteins for organizing "preassembled signaling complexes" at the plasma membrane. J. Biol. Chem. 273 (10), 5419–5422.

Olson, E.N., 1990. MyoD family: a paradigm for development? Genes Dev. 4 (9), 1454–1461.

Razandi, M., Oh, P., Pedram, A., Schnitzer, J., Levin, E.R., 2002. ERs associate with and regulate the production of caveolin: implications for signaling and cellular actions. Mol. Endocrinol. 16 (1), 100–115.

Rossouw, J.E., Anderson, G.L., Prentice, R.L., LaCroix, A.Z., Kooperberg, C., Stefanick, M.L., Jackson, R.D., Beresford, S.A., Howard, B.V., Johnson, K.C., Kotchen, J.M., Ockene, J., 2002. Risks and benefits of estrogen plus progestin in healthy postmenopausal women: principal results From the Women's Health Initiative randomized controlled trial. Jama 288 (3), 321–333.

Sanchez-Garcia, I., Rabbitts, T.H., 1994. The LIM domain: a new structural motif found in zinc-finger-like proteins. Trends Genet. 10 (9), 315–320.

Sartore, S., Chiavegato, A., Faggin, E., Franch, R., Puato, M., Ausoni, S., Pauletto, P., 2001. Contribution of Adventitial Fibroblasts to Neointima Formation and Vascular Remodeling: From Innocent Bystander to Active Participant. Circ. Res. 89, 1111–1121.

Schmeichel, K.L., Beckerle, M.C., 1994. The LIM domain is a modular protein-binding interface. Cell 79 (2), 211–219.

Schnitzer, J.E., Liu, J., Oh, P., 1995. Endothelial caveolae have the molecular transport machinery for vesicle budding, docking, and fusion including VAMP, NSF, SNAP, annexins, and GTPases. J. Biol. Chem. 270 (24), 14399–14404.

Severs, N.J., 1988. Caveolae: static inpocketings of the plasma membrane, dynamic vesicles or plain artifact? J. Cell Sci. 90 (Pt 3), 341–348.

Sudoh, N., Toba, K., Akishita, M., Ako, J., Hashimoto, M., Iijima, K., Kim, S., Liang, Y.Q., Ohike, Y., Watanabe, T., Yamazaki, I., Yoshizumi, M., Eto, M., Ouchi, Y., 2001. Estrogen prevents oxidative stress-induced endothelial cell apoptosis in rats. Circulation 103 (5), 724–729.

Sullivan Jr., T.R., Karas, R.H., Aronovitz, M., Faller, G.T., Ziar, J.P., Smith, J.J., O'Donnell Jr., T.F., Mendelsohn, M.E., 1995. Estrogen inhibits the response-to-injury in a mouse carotid artery model. J. Clin. Invest. 96 (5), 2482–2488.

Takeda-Matsubara, Y., Nakagami, H., Iwai, M., Cui, T.X., Shiuchi, T., Akishita, M., Nahmias, C., Ito, M., Horiuchi, M., 2002. Estrogen activates phosphatases and antagonizes growth-promoting effect of angiotensin II. Hypertension 39 (1), 41–45.

Watanabe, T., Yoshizumi, M., Akishita, M., Eto, M., Toba, K., Hashimoto, M., Nagano, K., Liang, Y.Q., Ohike, Y., Iijima, K., Sudoh, N., Kim, S., Nakaoka, T., Yamashita, N., Ako, J., Ouchi, Y., 2001. Induction of nuclear orphan receptor NGFI-B gene and apoptosis in rat vascular smooth muscle cells treated with pyrrolidinedithiocarbamate. Arterioscler Thromb. Vasc. Biol. 21 (11), 1738–1744.

Weisz, A., Bresciani, F., 1988. Estrogen induces expression of c-fos and c-myc protooncogenes in rat uterus. Mol. Endocrinol. 2 (9), 816–824.

5. Joutel A, Dodick DD, Parisi JE et al. De novo mutation in the NOTCH3 gene causing CADASIL. Ann Neurol 2000;47:388–391.
6. O'Riordan S, Nor AM, Hutchinson M. CADASIL imitating multiple sclerosis. The importance of MRI markers. Multiple Sclerosis 2002;5:430–432.
7. Engelter ST, Ruegg S, Kirsch EC et al. CADASIL mimicking primary angiitis of the central nervous system. Arch Neurol 2002;59:1480–1483.
8. van Den Boom R, Lesnick Oberstein SA, van Duinen SG et al. Subcortical lacunar lesions: An MR imaging finding in patients with cerebral autosomal dominant arteriopathy with subcortical infarcts and leukoencephalopathy. Radiology 2002;224:791–796.
9. Haley EC. Encephalopathy following arteriography: A possible toxic effect of contrast agents. Ann Neurol 1984;15:100–102.
10. Dichgans M, Petersen Angiographic complications in CADASIL. Lancet 1997;349:776–777.

CORRELATION BETWEEN PULSE WAVE VELOCITY AND COGNITIVE FUNCTION IN NONVASCULAR DEMENTIA

To The Editor: We read with interest the paper by Shimoda et al.[1] showing that pulse wave velocity (PWV), an indicator of arterial stiffness, was higher in patients with vascular dementia than in patients with Alzheimer's disease and nondemented control subjects. Vascular factors such as smoking, hypertension, diabetes mellitus, and apolipoprotein E ε4 allele have also been implicated in the development of nonvascular dementia, including Alzheimer's disease,[2] but there has been no quantitative study of the relationship between the stage of arteriosclerosis and the severity of nonvascular dementia. In this study, PWV was measured in patients with mild to moderate nonvascular dementia, and greater arterial stiffness was associated with cognitive impairment.

Patients who were referred to the Memory Clinic of our department were enrolled. Patients with definite vascular dementia such as poststroke patients and patients with multiple cerebral infarcts were excluded. Twenty-seven subjects (12 men and 15 women, mean age ± standard deviation = 76 ± 7) were analyzed, including 14 patients with Alzheimer's disease diagnosed using the *Diagnostic and Statistical Manual of Mental Disorders, Fourth Edition*, and others with mild cognitive impairment. PWV was measured using the automated device Form PWV/ABI (Colin Co. Ltd, Komaki, Japan), and two measurements, heart-brachial (hb) PWV and brachial-ankle (ba) PWV, were analyzed.[3] Cognitive function was assessed using the Hasegawa Dementia Scale Revised (HDSR; 20 ± 7 points out of 30). Basic activities of daily living (ADLs), instrumental ADLs, mood, and volition were also measured using the Barthel index, Lawton-Brody instrumental ADLs, Geriatric Depression Scale, and Vitality Index,[4] respectively.

In the analysis including all the subjects, HDSR correlated with hbPWV ($r = -0.450$, $P<.05$) (Figure 1) and baPWV ($r = -0.433$, $P<.05$), whereas other indices of the comprehensive geriatric assessment did not correlate with hbPWV or baPWV. Multiple regression analysis using HDSR as a dependent variable and hbPWV, age, sex, mean blood pressure, and use of antihypertensive agents as independent variables showed that hbPWV ($\beta = -0.535$, $P<.05$) was a significant determinant of HDSR. Analysis using systolic blood pressure instead of mean blood pressure showed a comparable result, but analysis using baPWV instead of hbPWV did not reach statistical significance.

Subjects were excluded because they had obvious vascular factors (n = 9), extensive white-matter lesions on brain magnetic resonance imaging scans (n = 5), or a history of hypertension (n = 8) as determined by the use of antihypertensive agents or blood pressure of 140/90 mmHg or higher. These subjects showed higher hbPWV than the other 18 subjects (665 ± 139 vs 561 ± 98 cm/s, $P<.05$) and lower HDSR score (15.6 ± 5.4 vs 21.9 ± 6.7, $P<.05$), whereas age was not significantly different (79 ± 9 vs 76 ± 7, $P=.29$). Then, the correlation between PWV and cognitive function was analyzed in the 18 subjects without vascular factors. In simple regression analysis, HDSR correlated with hbPWV ($r = -0.615$, $P<.01$) (Figure 1) and baPWV ($r = -0.618$, $P<.01$). Multiple regression analysis using HDSR as a dependent variable and hbPWV, age, sex, and mean blood pressure as independent variables revealed that hbPWV ($\beta = -0.700$, $P<.05$) was independently related to HDSR.

The present study demonstrated that subjects with extensive white-matter lesions or a history of hypertension had higher PWV than others, consistent with a previous report,[1] even though subjects with typical vascular dementia were excluded. Multivariate analysis and analysis using the subjects without obvious vascular factors showed that arterial stiffness as measured using PWV was independently related to cognitive function. These results suggest that arteriosclerosis, even in a subclinical state, plays a role in cognitive impairment and that PWV serves as a useful tool to assess the vascular contribution in subjects with mild to moderate nonvascular dementia. Recent papers have shown that PWV can predict the future occurrence of cardiovascular disease.[5] Furthermore, a new paradigm—vascular cognitive impairment—in which vascular factors play a variety of roles in the pathogenesis of dementia has been proposed.[2] It is necessary to perform a large-scale study to confirm our preliminary results and a prospective

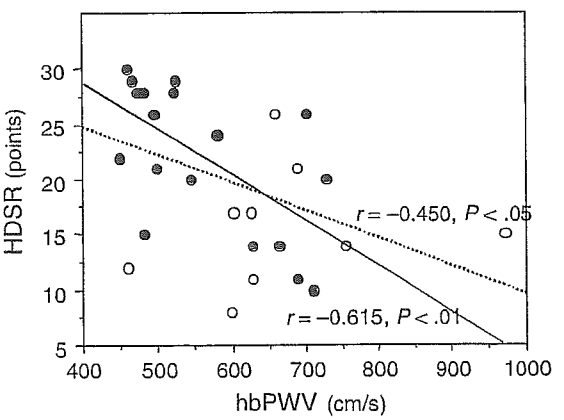

Figure 1. Correlation between heart-brachial pulse wave velocity (hbPWV) and Hasegawa Dementia Scale Revised (HDSR) in subjects with (open circles, n = 9) and without (closed circles, n = 18) vascular factors such as extensive white-matter lesions and history of hypertension. Dotted line and solid line indicate regression lines in all the subjects and the subjects without vascular factors, respectively.

longitudinal study to examine whether high PWV could be a risk factor for cognitive impairment.

Kumiko Nagai, MT
Masahiro Akishita, MD
Ayako Machida, CSLP
Kazuki Sonohara, MD
Mitsuo Ohni, MD
Kenji Toba, MD
Department of Geriatric Medicine
Kyorin University School of Medicine
Tokyo, Japan

REFERENCES

1. Shimoda H, Mizushima Y, Oobasawa H et al. Pulse wave velocity in persons with vascular dementia. J Am Geriatr Soc 2003;51:1329–1330.
2. O'Brien JT, Erkinjuntti T, Reisberg B et al. Vascular cognitive impairment. Lancet Neurol 2003;2:89–98.
3. Yamashina A, Tomiyama H, Takeda K et al. Validity, reproducibility, and clinical significance of noninvasive brachial-ankle pulse wave velocity measurement. Hypertens Res 2002;25:359–364.
4. Toba K, Nakai R, Akishita M et al. Vitality Index as a useful tool to assess elderly with dementia. Geriatr Gerontol Int 2002;2:23–29.
5. Boutouyrie P, Tropeano AI, Asmar R et al. Aortic stiffness is an independent predictor of primary coronary events in hypertensive patients: A longitudinal study. Hypertension 2002;39:10–15.

GERIATRIC TRAINING IN PROBLEM-BASED LEARNING: AN ASIAN PERSPECTIVE

To the Editor: Problem-based learning (PBL) is gradually becoming popular in medical schools in Asian countries.[1] It is an integrated, student-centered educational approach, which uses problems (triggers) as the key units for stimulating and structuring relevant student learning. Such learning is largely dependent on the quality of the problems[2] and the areas tested in PBL.[3] Aligning PBL activities with subsequent student assessment often proves to be difficult, because it is different from the assessment conducted in the traditional curriculum. A study was conducted to analyze the PBL problems and examination questions used in the School of Medical Sciences, Universiti Sains Malaysia (USM) to examine the demographic characteristics of the people featured and the level of acuity of case scenarios presented.

All PBL problems (n = 51) used in Phase II (Years 2 and 3) of USM PBL curriculum, 95 modified essay questions (MEQ), and 169 objective-structured clinical examination (OSCE) questions (in which age and presenting illness were mentioned) of five academic sessions (1998–2003) were analyzed. The findings revealed that problems and examination questions mostly included acute and rapidly resolving illnesses in young people and underemphasized elderly people (aged $\geq$60) with chronic, irreversible diseases. Only nine (17%) problems and 34 examination questions (MEQ 19%, OSCE 10%) featured older people. Moreover, those problems and questions mainly involved the early elderly (aged 60–74). Only one problem and one MEQ featured advanced elderly (aged $\geq$70). In the problems and questions, where the presenting illness was mentioned, it was of one month's duration in 78% of problems, 69% of MEQs, and 41% of OSCEs. Conversely, only in 4% of problems, 8% of MEQs, and 22% of OSCEs, was the presenting complaint of more than 1 year's duration. In 41 PBL problems, the outcome was mentioned; this occurred within 1 year in 11%, within 1 month in 28%, and within 1 week in 61%.

Adequate exposure to geriatric-related issues is provided to the students in the different phases of the USM curriculum. As the PBL is the main teaching–learning strategy in Phase 2 that facilitates the integration of basic and clinical sciences, such emphasis may contribute to the development of negative attitudes among the students toward elderly patients and people with chronic diseases, as mentioned in other studies.[4,5] Studies also showed that this type of emphasis might also deter students from careers that focus on the elderly[6] and chronically sick.[7] This has wider implications when there is a clear demographic trend toward a rapid increase of the elderly population in Malaysia and worldwide.[8] According to United Nations estimates, the population of elderly in the world will reach 1.2 billion by 2025, the majority of whom will be in developing countries.[9] This is also important because health care is shifting away from the diagnosis and management of acute diseases toward caring for increasingly elderly people with chronic illnesses.[8]

As a subject, geriatric medicine is not well established in the schools of Asian countries. The World Health Organization[8] strongly advocated including relevant aging- and geriatric-related issues in the medical curriculum. Medical schools should provide opportunities for their students to be exposed to older patients with adequate positive experiences in hospital, community, and long-term care settings. Some problems of the PBL segment and examination questions could be designed to focus exclusively on the elderly with chronic diseases.[10] Curriculum planners should regularly analyze the demographic and pedagogical characteristics of problems and examination questions to determine whether aging- and geriatric-related content is adequately covered in PBL curriculum. Emphasis given to such content significantly improves attitudes and knowledge of students toward the elderly.[4] Reorientation of medical education is necessary to promote more concern among physicians about the needs of the elderly and people who are chronically ill.

Md. Anwarul Azim Majumder, PhD
Ahmed Fuad Ab. Rahim, MHPEd
Department of Medical Education
Sayeeda Rahman, MPharm, MBA
Department of Pharmacology
School of Medical Sciences
Universiti Sains Malaysia
Kelantan, Malaysia

REFERENCES

1. Khoo HE. Implementation of problem-based learning in Asian medical schools and students' perceptions of their experience. Med Educ 2003;37:401–409.
2. Schmidt HG, Dolmans D, Gijselaers WH et al. Theory-guided design of rating scale for course evaluation in problem-based curricula. Teach Learn Med 1995;7:82–91.
3. Connolly C, Seneque M. Evaluating problem-based learning in multilingual student population. Med Educ 1999;33:738–744.
4. Shahidi S, Devlen J. Medical students' attitudes and knowledge of the aged. Med Educ 1993;27:286–288.

ELSEVIER

Atherosclerosis 173 (2004) 13–18

ATHEROSCLEROSIS

www.elsevier.com/locate/atherosclerosis

Interrelationship between non-invasive measurements of atherosclerosis: flow-mediated dilation of brachial artery, carotid intima-media thickness and pulse wave velocity

Kumiko Kobayashi[a], Masahiro Akishita[a,*], Wei Yu[a], Masayoshi Hashimoto[b], Mitsuo Ohni[a], Kenji Toba[a]

[a] *Department of Geriatric Medicine, Kyorin University School of Medicine, 6-20-2 Shinkawa, Mitaka, Tokyo 181-8611, Japan*
[b] *Department of General Internal Medicine, Kobe University School of Medicine, Kobe, Japan*

Received 10 April 2003; received in revised form 11 August 2003; accepted 30 October 2003

Abstract

Flow-mediated dilation (FMD) of the brachial artery, carotid intima-media thickness (IMT) and pulse wave velocity (PWV) have been shown to be good surrogate markers of clinical atherosclerosis. We determined the interrelation between these measurements, and examined whether their combination would be of clinical significance. One hundred and thirty-five consecutive subjects (79 women/56 men) were enrolled, including 110 patients with risk factors for atherosclerosis, and 33 patients with atherosclerotic disease such as coronary heart disease, stroke or arteriosclerosis obliterans. IMT and plaque formation of the carotid artery and FMD of the brachial artery were assessed using ultrasonography. Brachial-ankle PWV (baPWV) was measured using an automated device (form ABI/PWV, Colin). Age, FMD, IMT and PWV were significantly correlated with each other. Multivariate analysis revealed an independent correlation between the parameters except for FMD, and all four parameters were independently correlated with each other in subjects <70 years. Next, we classified the subjects by tertile according to the values of FMD, IMT and PWV. Each of the worst tertiles was associated with a higher prevalence of atherosclerotic disease and carotid plaques compared to the other tertiles. Moreover, subjects with the worst tertiles of all three measurements had a markedly higher prevalence of atherosclerotic disease and carotid plaques. These results suggest that FMD, IMT and PWV are related to each other, but the combination of these measurements will be of stronger clinical relevance.

Keywords: Arteriosclerosis; Endothelium; Arterial stiffness; Elasticity

1. Introduction

A number of methods have been applied for the non-invasive assessment of cardiovascular risks. These include flow-mediated dilation (FMD) of the brachial artery, pulse wave velocity (PWV) and carotid intima-media thickness (IMT). FMD is known to be endothelium-dependent and can be measured during reactive hyperemia using high-resolution ultrasound [1,2]. Measurement of IMT also employs B-mode ultrasonography, which can detect morphological change of the carotid artery, consisting of both an intimal atherosclerotic process and medial hypertrophy [3]. PWV reflects arterial distensibility and can be measured by pressure or volume pulse wave analysis using a transducer [4]. These three methods have been widely used in clinical settings because they are shown to be good surrogate markers of clinical atherosclerosis [1–4]. Impairment of these indices is associated with coronary artery disease or cerebrovascular disease. Also, in patients with atherosclerosis risk factors such as hypertension, hyperlipidemia and diabetes mellitus, each of these three indices is impaired and can be ameliorated by treatment [1–4].

Several studies have demonstrated a significant correlation between aortic PWV and carotid IMT [5,6]. We have previously shown that FMD was negatively correlated with IMT [7]. However, little data have been published on the interrelation of these three measurements. In addition, whether their combination is clinically significant and useful has not been elucidated.

* Corresponding author. Tel.: +81-422-47-5511; fax: +81-422-44-1917.
E-mail address: akishita@kyorin-u.ac.jp (M. Akishita).

0021-9150/$ – see front matter © 2003 Elsevier Ireland Ltd. All rights reserved.
doi:10.1016/j.atherosclerosis.2003.10.013

In the present study, we demonstrated that decreased FMD in the brachial artery was related to increased brachial-ankle and heart-carotid PWV (hcPWV) as well as to increased carotid IMT. Furthermore, we showed that the combination of these three measurements was useful in predicting the presence of atherosclerotic disease.

2. Methods

2.1. Subjects

One hundred and thirty five consecutive subjects were enrolled in this study. The characteristics of the study subjects are shown in Table 1. They included 25 healthy volunteers, 110 patients with atherosclerosis risk factors such as hypertension, hyperlipidemia or diabetes mellitus, and 33 patients with atherosclerotic disease such as coronary heart disease, stroke or arteriosclerosis obliterans. They were recruited from outpatients, inpatients, and community volunteers. A history was taken, and physical examination and laboratory tests were performed in all subjects. Atherosclerotic disease was defined as follows: (1) stroke, confirmed by brain computed tomography and a documented history; (2) coronary artery disease, confirmed by coronary arteriography and/or a documented history of myocardial infarction within 5 years; (3) a clinical diagnosis of arteriosclerosis obliterans. Exclusion criteria for this study included clinical manifestations of venous thromboembolism, liver disorder and history of cancer(s). Each subject gave written informed consent before enrollment in this study, after receiving a thorough explanation of the study design and protocol.

Table 1
Clinical characteristics of subjects and classification by tertile of atherosclerotic measures

Men/women	56/79 ($n = 135$)
Age (years)	62 ± 16
No risk factor, *n* (%)	25 (19)
Hypertension, *n* (%)	51 (38)
Hyperlipidemia, *n* (%)	64 (47)
Diabetes mellitus, *n* (%)	35 (26)
Current smoker, *n* (%)	20 (15)
Atherosclerotic disease	
Stroke, *n* (%)	21 (16)
Coronary artery disease, *n* (%)	10 (7)
Arteriosclerosis obliterans, *n* (%)	5 (4)
Total atherosclerotic disease, *n* (%)	33 (24)
Atherosclerotic measurements	
FMD (%)	
Tertile 1 (≥4.0)	6.0 ± 1.7
Tertile 2 (≥1.9, <4.0)	2.9 ± 0.7
Tertile 3 (<1.9)	0.8 ± 0.9
IMT (mm)	
Tertile 1 (<0.75)	0.63 ± 0.08
Tertile 2 (≥0.75, <1.02)	0.87 ± 0.11
Tertile 3 (≥1.02)	1.17 ± 0.19
baPWV (m/s)	
Tertile 1 (<14.34)	12.37 ± 1.40
Tertile 2 (≥14.34, <18.80)	16.18 ± 1.26
Tertile 3 (≥18.80)	22.88 ± 3.99
hcPWV (m/s)	
Tertile 1 (<7.40)	6.00 ± 1.04
Tertile 2 (≥7.40, <9.80)	8.53 ± 0.73
Tertile 3 (≥9.80)	11.56 ± 1.65

Age and atherosclerotic measurements by tertile are expressed as mean ± S.D. FMD, percent flow-mediated dilation of brachial artery; IMT, intima-media thickness of common carotid artery; baPWV and hcPWV, brachial-ankle and heart-carotid pulse wave velocity, respectively.

2.2. Measurement of carotid IMT

Ultrasound measurements of IMT of the common carotid artery were performed as previously described [7] by an examiner who was unaware of the subjects' clinical background. The same examiner performed the measurements of IMT, FMD and PWV throughout the study. Briefly, IMT was measured from high-resolution, two-dimensional ultrasound images obtained with an ultrasound machine (PowerVision 6000, Toshiba) with a 7.5 MHz linear-array transducer. The subject reclined on the examination table for 15 min before the initial carotid ultrasound scanning, in a quiet, temperature-controlled (22–24 °C) room. This measurement was applied to the far wall of the right carotid artery. With the subject in the supine position, an ultrasound probe was applied longitudinally to the surface of the skin on the right side of the neck. Longitudinal scanning was performed from the common carotid artery to the bifurcation of the common carotid artery. Scanning was performed in the optimal position. An ECG monitor integrated with the ultrasound machine was also applied. The ultrasound images were recorded on S-VHS videotape. After the bifurcation of the common carotid artery was confirmed, IMT was measured from the B-mode scan with electronic calipers to within 10 mm proximal to the bifurcation. Four points were measured in one scan, which was synchronized with the R-wave peaks on the ECG to avoid possible errors resulting from variable arterial compliance. Two scans were performed for each study subject. Mean IMT was calculated from eight points. The variability of the ultrasound measurements of IMT was studied by performing five measurements over 1 month in 12 volunteers. The intraobserver coefficient of variation for measurement of IMT was 4.2 ± 0.7%.

The presence of plaque(s) in the right carotid artery was assessed by evaluating the ultrasound images of the common and internal carotid artery, and the bifurcation. A plaque was defined as a focal widening relative to adjacent segments, with protrusion into the lumen composed of either only calcified deposits or a combination of calcified and non-calcified material [5].

2.3. Measurement of FMD of brachial artery

Studies of FMD were performed according to the method described previously [7]. The diameter of the artery was

measured on high-resolution, two-dimensional ultrasound images obtained with an ultrasound machine (PowerVision 6000, Toshiba) with a 7.5 MHz linear-array transducer. Machine operating parameters were kept constant during each study.

The right brachial artery was scanned over a longitudinal section, 3–5 cm above the right elbow. Depth and gain settings were optimized to identify the lumen-to-vessel wall interface. An ECG monitor integrated with the ultrasound machine was also applied. When an adequate image was obtained, the surface of the skin was marked, and the arm was kept in the same position throughout the study. A pneumatic tourniquet placed around the forearm distal to the target artery was inflated to a pressure of 250 mmHg, and inflation was held for 5 min. Increased flow was then induced by sudden cuff deflation. A second scan was performed continuously for 60 s before and 120 s after cuff deflation. The ultrasound images were recorded on S-VHS videotape. The diameter of the brachial artery was measured from the anterior to the posterior interface between the media and adventitia ("m line") at a fixed distance. The mean diameter was calculated from four cardiac cycles synchronized with the R-wave peaks on the ECG. All measurements were made at end-diastole to avoid possible errors resulting from variable arterial compliance. Maximal vasodilatation was observed 45–60 s after cuff release. The change in diameter caused by FMD was expressed as the percent change relative to that in the initial resting scan. The velocity profile of blood flow was simultaneously recorded. Mean flow velocity was calculated by measuring the area under this velocity profile curve. Blood flow (in milliliters per minute) was then calculated by multiplying the cross-sectional area of the brachial artery, which was based on the diameter, and the mean flow velocity. Changes in diameter of 0.1–0.2 mm can be detected accurately with this method [7]. The intraobserver coefficient of variation for measurements of FMD was 5.8 ± 0.3% (10 measurements in five subjects).

2.4. Measurement of PWV

PWV measurements were performed subsequently to FMD measurements, with the subject in the supine position. PWV was measured using an automated device (form PWV/ABI, Colin Co. Ltd., Komaki, Japan) as previously reported [8,9]. The device records PWV, blood pressure, ECG and heart sounds simultaneously. ECG electrodes were placed on both wrists, and a heart sound microphone was placed on the left sternal border.

The cuffs to measure brachial-ankle PWV (baPWV) were wrapped around both upper arms and ankles, and connected to a plethysmographic sensor that determines volume pulse form. Volume waveforms were stored for a sampling time of 10 s with automatic gain analysis and quality adjustment. The time delay from the ascending point of the right brachial waveform to the ascending point of each ankle waveform (ΔTba) was determined. The distance of each segment (Lb-La) is automatically calculated based on the patient's height and was derived from statistical studies. Then, baPWV was calculated using the formula; baPWV = La-Lb/ΔTba. The average of left and right baPWV in each subject was used for the analysis. To measure heart-carotid PWV, a multi-element carotid tonometry sensor with a holder arm was placed around the neck [9]. The time delay from the foot of the second sound of the phonocardiogram to the dicrotic notch of the carotid waveform (ΔThc) was calculated. The distance from the heart to the carotid artery (Lc) was deduced based on the patient's height. Then, hcPWV was calculated using the formula; hcPWV = Lc/ΔThc. The intraobserver coefficients of variation for measurements of baPWV and hcPWV were 2.0 ± 0.5 and 4.5 ± 1.4%, respectively (five measurements in eight subjects).

2.5. Statistical analysis

All data in the text, tables, and figures are expressed as mean ± S.E.M. unless otherwise specified. Pearson's simple correlation coefficient between age, FMD, IMT and PWV was determined. Categorical difference was analyzed by Chi-squared test. Standardized regression coefficients from multiple regression analysis of baPWV in relation to age, FMD and IMT were analyzed. Logistic regression analysis was performed to evaluate the relation between the combination of FMD, IMT and PWV, and the prevalence of atherosclerotic disease and carotid plaques. A value of $P < 0.05$ was considered statistically significant.

3. Results

3.1. Correlation between age, FMD, IMT and PWV

Table 2 shows the Pearson correlation matrix between age, FMD, IMT, baPWV and hcPWV. All the parameters were significantly correlated with each other. However, each subject did not always belong to the same category by tertile of atherosclerotic measurements (Fig. 1); e.g., the subjects in tertile 3 of baPWV (baPWV ≥ 18.80) were widely distributed in the tertiles of FMD; conversely, the subjects in

Table 2
Pearson correlation matrix between age, FMD, IMT and PWV

	FMD	IMT	baPWV	hcPWV
Age	−0.592	0.567	0.662	0.478
FMD		−0.343	−0.493	−0.364
IMT			0.477	0.460
baPWV				0.392

FMD, percent flow-mediated dilation of brachial artery; IMT, intima-media thickness of common carotid artery; baPWV and hcPWV, brachial-ankle and heart-carotid pulse wave velocity, respectively. All correlation coefficients were statistically significant ($P < 0.0001$).

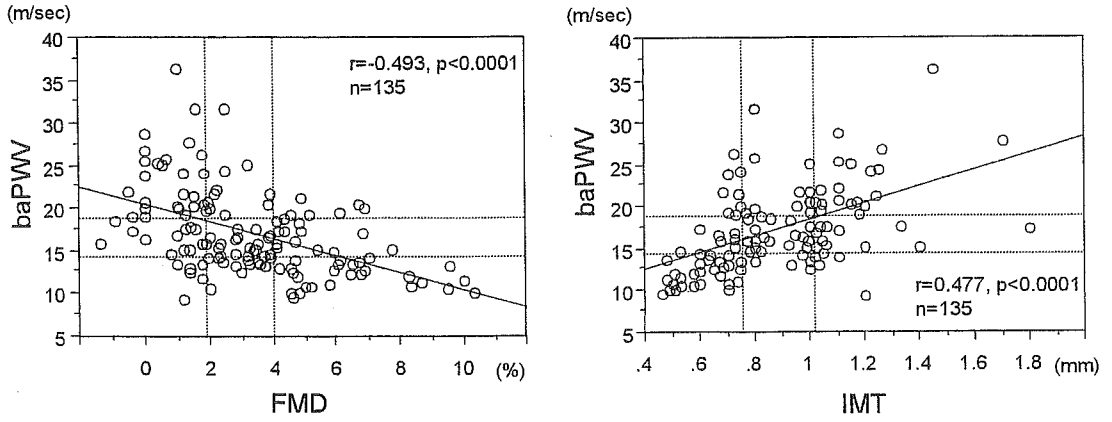

Fig. 1. Relations between brachial-ankle PWV (baPWV) and flow-mediated dilation (FMD) of brachial artery (left panel), and between baPWV and carotid intima-media thickness (IMT) (right panel). Solid lines and dotted lines indicate regression lines and tertile borders of each measurement, respectively.

tertile 3 of FMD (FMD $\leq$ 1.9) were widely distributed in the tertiles of baPWV.

Multiple regression analysis was performed with baPWV as a dependent variable and with age, mean arterial pressure of the right brachium, FMD and IMT as independent variables. As shown in Table 3, age, mean arterial pressure and IMT were independently related to baPWV. If the subjects <70 years (n = 89) were analyzed separately to diminish the effect of age, FMD as well as IMT, mean arterial pressure and age were independent determinants of baPWV. Multiple regression analysis with FMD or IMT as a dependent variable and analysis using hcPWV instead of baPWV showed comparable results.

3.2. Prevalence of atherosclerotic disease and carotid plaques in relation to FMD, IMT and PWV

We classified the subjects by tertile according to the values of FMD, IMT and baPWV (Table 1). Each of the worst tertiles, tertile 3, was associated with a higher prevalence of atherosclerotic disease and carotid plaques compared to the other tertiles. Atherosclerotic disease was found in 36, 40 and 39% of subjects in tertile 3 of FMD, IMT and baPWV, respectively, but was found in 18, 15 and 16% of subjects in the other tertiles of the corresponding parameter ($P < 0.05$ by Chi-squared test). Similarly, carotid plaques were found in 64, 70 and 69% of subjects in tertile 3 of FMD, IMT and baPWV, respectively, but in 34, 28 and 30% of subjects in the other tertiles of the corresponding parameter ($P < 0.01$ by Chi-squared test). These results suggest that each of the three measurements is comparably predictive of atherosclerotic disease and carotid plaques. As shown in Fig. 2, however, the subjects with the worst tertiles of all three measurements had a markedly higher prevalence of atherosclerotic disease and carotid plaques (67 and 89%, respectively). In logistic regression analysis unadjusted or adjusted for sex, hypertension, hyperlipidemia, diabetes and current smoking, the number of worst tertiles was signif-

Table 3
Multiple regression analysis with brachial-ankle PWV as dependent variable and age, mean arterial pressure (MAP), FMD and IMT as independent variables

	All subjects		Age <70 years	
	R	P-value	R	P-value
Age	0.406	0.000	0.245	0.022
MAP	0.261	0.000	0.215	0.009
FMD	−0.130	0.110	−0.212	0.025
IMT	0.169	0.027	0.336	0.000

R represents standardized regression coefficients. FMD, percent flow-mediated dilation of brachial artery; IMT, intima-media thickness of common carotid artery and PWV, brachial-ankle pulse wave velocity.

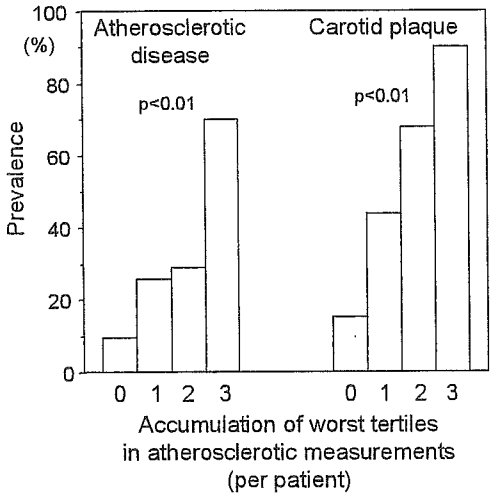

Fig. 2. Prevalence of atherosclerotic disease and carotid plaques according to the accumulation of worst tertiles in atherosclerotic measurements. Scores were recorded by counting how many measurements were in the worst tertiles in each patient. Atherosclerotic disease includes stroke, coronary artery disease and arteriosclerosis obliterans. Statistical analysis between the groups was performed by Chi-squared test and logistic regression analysis.

icantly related to the prevalence of atherosclerotic disease and carotid plaques; adjusted hazard ratio (95% confidence interval) by increment of the number of worst tertiles was 1.88 (1.13–3.13) for atherosclerotic disease and 3.37 (2.00–5.70) for carotid plaques. Accordingly, it is likely that the combination of FMD, IMT and PWV serves as a more accurate indicator of clinical atherosclerosis than any single measurement.

4. Discussion

Endothelial dysfunction is an early and potentially reversible event in atherogenesis [10], being detected as a decrease in FMD of the brachial artery [1,2]. An increase in PWV reflects arterial stiffening as a result of structural and functional changes of the vascular tree [4]. Recent reports have demonstrated that endothelial nitric oxide is also implicated in the regulation of PWV [11,12]. In contrast, carotid IMT quantitatively measures the arterial morphology consisting of intimal lesions and medial hypertrophy [3]. Consequently, brachial FMD, carotid IMT and brachial-ankle or heart-carotid PWV evaluates different aspects of atherosclerosis as well as different sites of the artery. Atherosclerosis, however, undergoes systemic progression and results in the worsening of these atherosclerotic parameters to some extent. Taken together, it is reasonable that FMD, IMT and PWV correlated with each other in this study. This result implies that each of the three measurements would be clinically useful in a cohort study investigating the effect of intervention therapy on outcomes.

When applying FMD, IMT and PWV to the clinical setting, a problem may exist concerning the variability between the three measurements on an individual basis. A good or bad result of a single measurement may mislead the clinical evaluation of a subject. An important issue is how these atherosclerotic parameters can predict the future occurrence of cardiovascular events, and should be addressed by prospective studies. Although each of FMD [13], IMT [14] and PWV [15] is reported to be predictive of cardiovascular events, the significance of their combination has not been determined. Alternatively, we used the existence of atherosclerotic disease and carotid plaques as surrogate atherosclerotic outcomes, and tested the hypothesis that the accumulation of inferior results would be associated with higher rates of these outcomes. Analysis by tertile showed that the combined evaluation of FMD, IMT and PWV highly detected the prevalence of atherosclerotic disease and carotid plaques compared to single assessment. Therefore, accuracy may be improved by combining these three measurements.

Combination of FMD, IMT and PWV may give reliable information on clinical or subclinical atherosclerosis, but bears the burden of time and manpower. Particularly, measurement of FMD requires more than half an hour, as well as skill for examination and measurement. Also, inter-observer or inter-institutional variation in FMD [2] may make it difficult to repeat measurements in a patient over years. In contrast, IMT and PWV seem less complicated in terms of examination time and procedure [3,4]. The automated device for the measurement of PWV used in the present study requires only a few minutes for the whole procedure [8]. Thus, PWV and/or IMT may be appropriate for the screening of patients with atherosclerosis risk factors and for large-scale studies. As a non-invasive assessment of endothelial function, however, FMD will remain the gold standard until alternative simple and objective methods are established. Because some subjects have endothelial dysfunction before developing atherosclerosis that can be measured by IMT and PWV, it is important to evaluate endothelial function as well.

This study contains some limitations in interpreting the data. Brachial-ankle PWV is not so familiar as conventional carotid-femoral and heart-ankle PWV, and its significance for the prediction of cardiovascular events has not been published. However, the validity and reliability of brachial-ankle PWV are defined using the same device as ours [8,16]. We also confirmed using the present samples that brachial-ankle PWV was correlated well with heart-ankle PWV ($r = 0.859$). Our device estimates the path length from the height of each subject based on the superficial measurements in a Japanese population, suggesting possible errors. However, use of the equation should not seriously harm the reliability of PWV measurements because Pearson's correlation coefficient between the estimated length and the actual surface measurement was higher than 0.9 (unpublished results). At the time of FMD measurement, we did not administer nitroglycerin to the study subjects in order to avoid adverse reactions. Accordingly, we could not separate endothelium-independent dilation from endothelium-dependent dilation. In addition, to collect a sufficient number of subjects with different stages of atherosclerosis, miscellaneous subjects were included such as healthy young volunteers and older patients with atherosclerotic disease. Most of the subjects had atherosclerosis risk factors and were taking some drugs for its treatment. Because these factors influence FMD, IMT and PWV [1–4], it is possible that the disease and/or medication may have affected the relationship between the measurements. Consequently, the results of the present study should be confirmed in subjects without medication and without risk factors. In addition, we used the presence of atherosclerotic disease and carotid plaques as surrogate atherosclerotic outcomes, and showed that the accumulation of inferior results was associated with higher rates of these outcomes. This should be confirmed by prospective studies examining the future occurrence of cardiovascular events.

In conclusion, FMD of the brachial artery, carotid IMT, and brachial-ankle and heart-carotid PWV were related to each other. Combination of the three methods was useful in predicting the burden of atherosclerosis, and is thus of clinical relevance.

Acknowledgements

This study was supported by Health and Labour Sciences Research Grants (H14-kossetu-019, H14-kouka (seikatu)-014, H15-Choju-013 and H15-Choju-015) from the Ministry of Health, Labour and Welfare of Japan.

References

[1] Behrendt D, Ganz P. Endothelial function. From vascular biology to clinical applications. Am J Cardiol 2002;90:40L–8L.
[2] Raitakari OT, Celermajer DS. Flow-mediated dilatation. Br J Clin Pharmacol 2000;50:397–404.
[3] Simon A, Gariepy J, Chironi G, Megnien JL, Levenson J. Intima-media thickness: a new tool for diagnosis and treatment of cardiovascular risk. J Hypertens 2002;20:159–69.
[4] O'Rourke MF, Mancia G. Arterial stiffness. J Hypertens 1999;17:1–4.
[5] van Popele NM, Grobbee DE, Bots ML, Asmar R, Topouchian J, Reneman RS, et al. Association between arterial stiffness and atherosclerosis: the Rotterdam Study. Stroke 2001;32:454–60.
[6] Mackey RH, Sutton-Tyrrell K, Vaitkevicius PV, Sakkinen PA, Lyles MF, Spurgeon HA, et al. Correlates of aortic stiffness in elderly individuals: a subgroup of the Cardiovascular Health Study. Am J Hypertens 2002;15:16–23.
[7] Hashimoto M, Eto M, Akishita M, Kozaki K, Ako J, Iijima K, et al. Correlation between flow-mediated vasodilatation of the brachial artery and intima-media thickness in the carotid artery in men. Arterioscler Thromb Vasc Biol 1999;19:2795–800.
[8] Yamashina A, Tomiyama H, Takeda K, Tsuda H, Arai T, Hirose K, et al. Validity, reproducibility, and clinical significance of noninvasive brachial-ankle pulse wave velocity measurement. Hypertens Res 2002;25:359–64.
[9] Narimatsu K, Takatani S, Ohmori K. A multi-element carotid tonometry sensor for non-invasive measurement of pulse wave velocity. Front Med Biol Eng 2001;11:45–58.
[10] Ross R. The pathogenesis of atherosclerosis: a perspective for the 1990s. Nature 1993;362:801–9.
[11] Kinlay S, Creager MA, Fukumoto M, Hikita H, Fang JC, Selwyn AP, et al. Endothelium-derived nitric oxide regulates arterial elasticity in human arteries in vivo. Hypertension 2001;38:1049–53.
[12] Wilkinson IB, Qasem A, McEniery CM, Webb DJ, Avolio AP, Cockcroft JR. Nitric oxide regulates local arterial distensibility in vivo. Circulation 2002;105:213–7.
[13] Neunteufl T, Heher S, Katzenschlager R, Wolfl G, Kostner K, Maurer G, et al. Late prognostic value of flow-mediated dilation in the brachial artery of patients with chest pain. Am J Cardiol 2000;86:207–10.
[14] O'Leary DH, Polak JF, Kronmal RA, Manolio TA, Burke GL, Wolfson Jr SK. Carotid-artery intima and media thickness as a risk factor for myocardial infarction and stroke in older adults. Cardiovasc Health Stud Collaborative Res Group N Engl J Med 1999;340:14–22.
[15] Boutouyrie P, Tropeano AI, Asmar R, Gautier I, Benetos A, Lacolley P, et al. Aortic stiffness is an independent predictor of primary coronary events in hypertensive patients: a longitudinal study. Hypertension 2002;39:10–5.
[16] Munakata M, Ito N, Nunokawa T, Yoshinaga K. Utility of automated brachial ankle pulse wave velocity measurements in hypertensive patients. Am J Hypertens 2003;16:653–7.

Original Article

Reduced Endothelial Vasomotor Function and Enhanced Neointimal Formation after Vascular Injury in a Rat Model of Blood Pressure Lability

Masato ETO, Kenji TOBA, Masahiro AKISHITA, Koichi KOZAKI, Tokumitsu WATANABE, Seungbum KIM, Masayoshi HASHIMOTO, Noriko SUDOH, Masao YOSHIZUMI, and Yasuyoshi OUCHI

Increased short-term blood pressure variability is known to be associated with hypertensive target organ damage. Sinoaortic denervation (SAD) induces a marked increase in blood pressure lability without affecting the average blood pressure level. The aim of this study was to investigate the effects of blood pressure lability on endothelial vasomotor function and neointimal formation after balloon injury in SAD rats. Direct long-term measurement of mean arterial pressure showed no significant difference in the average of mean arterial pressure between the SAD group and sham-operated control group. In contrast, the standard deviation of mean arterial pressure, as an index of blood pressure lability, was 3-fold greater in SAD rats. To study endothelial function, isometric tension of aortic rings was measured 4 weeks after SAD or sham operation. Endothelium-dependent vasorelaxation induced by acetylcholine was significantly reduced in the SAD group (20% reduction at maximum relaxation). Endothelium-independent vasorelaxation induced by sodium nitroprusside was similar in each group. Acetylcholine-induced NO release from aortic rings was significantly reduced in the SAD group. Next, we examined neointimal formation in carotid arteries in SAD and sham-operated rats at 2 weeks after balloon injury. The neointimal-to-medial area ratio in the SAD group was 50% higher than that in the sham-operated group. The percentage of proliferating cell nuclear antigen-positive cells in the intima was significantly higher in the SAD group. These findings suggest that increased blood pressure lability, independently of average blood pressure level, impairs endothelial function by inhibiting NO production, enhances neointimal formation after balloon injury, and may thereby contribute to atherogenesis. (*Hypertens Res* 2003; 26: 991–998)

***Key Words*: blood pressure lability, sinoaortic denervation, endothelial vasomotor function, neointimal formation, growth factor**

Introduction

It has been well established that hypertension is one of the most important risk factors for cardiovascular disease (*1*). The goal of treatment of hypertensive patients is not only to lower blood pressure but also to prevent cardiovascular events. In recent years, 24-h ambulatory blood pressure monitoring has become extensively used in clinical practice, and lines of evidence supporting its clinical value to predict hypertensive target organ damage and cardiovascular events have accumulated (*2*, *3*). It has been reported that the aver-

From the Department of Geriatric Medicine, Graduate School of Medicine, University of Tokyo, Tokyo, Japan.

This work was supported in part by a Grant-in-Aid (No. 08670768) for Scientific Research from the Ministry of Education, Science and Culture of Japan.

Address for Reprints: Yasuyoshi Ouchi, M.D., Ph.D., Department of Geriatric Medicine, Graduate School of Medicine, University of Tokyo, 7-3-1 Hongo, Bunkyo-ku, Tokyo 113-8655, Japan. E-mail: youchi-tky@umin.ac.jp

Received March 28, 2003; Accepted in revised form August 29, 2003.

age 24-h blood pressure level is significantly associated with cardiovascular damage, whereas the office blood pressure level is not (*2*). It has also been reported that an absence of nocturnal blood pressure fall (non-dipper phenomenon) is associated with cerebrovascular damage (*4*), whereas blood pressure lability, which is defined as increased short-term blood pressure variability and is a feature of hypertension in the elderly (*5*, *6*), has been reported to be associated with hypertensive target organ damage (*7*, *8*). However, the causal relationship between blood pressure lability and hypertensive organ damage remains unknown. To clarify this point, the direct effects of blood pressure lability on the vascular wall independent of the average blood pressure level should be investigated.

For this purpose, we selected sinoaortic-denervated rats as an animal model of blood pressure lability. The arterial baroreflex plays a pivotal role in the neural regulation of blood pressure. The afferent fibers of this negative feedback reflex arise from the carotid sinuses and aortic arch. Denervation of the afferent fibers of the baroreflex (sinoaortic denervation; SAD) was originally reported to induce neurogenic hypertension in rats (*9*). However, several studies using long-term continuous blood pressure measurement in the conscious state have shown that SAD does not affect the average blood pressure level and induces a marked increase in blood pressure variability (*10*, *11*).

The aim of this study was thus to elucidate the effects of blood pressure lability on vascular function and remodeling in SAD rats. In the first experiment, we examined the isometric tension of isolated aortic rings to investigate endothelial vasomotor function. In the second experiment, the degree of neointimal formation after balloon injury of the carotid artery was analyzed.

Methods

SAD Procedure

Ten-week-old male Wistar rats (Japan Clea, Tokyo, Japan) were used in this study. They were kept individually in stainless steel cages in a room where lighting was controlled (12 h on, 12 h off) and room temperature was maintained at around 22 °C. They were given a standard diet and water *ad libitum*. The experimental protocols were approved by the Animal Research Committee of the University of Tokyo. SAD was performed according to the method of Krieger with slight modification (*9*). Briefly, rats were anesthetized with a single intraperitoneal injection of pentobarbital (50 mg/kg). A midline neck incision was made and the sternocleidomastoid muscle was retracted laterally. The cervical sympathetic trunks, the superior laryngeal nerves and the aortic depressor nerves were bilaterally isolated and resected. The carotid sinuses were stripped of all connective tissue and treated with 10% phenol. After this procedure was completed, the incision was sutured. Sham-operated rats underwent the same procedure except that afferent fibers of the baroreflex were not denervated.

Continuous Mean Arterial Pressure (MAP) Recording

The femoral artery and vein were catheterized with polyethylene tubes (PE-50 and PE-20, respectively; Becton Dickinson, Parsippany, USA). To confirm denervation, baroreflex sensitivity was evaluated after intravenous bolus injection of phenylephrine hydrochloride (6 mg/kg). MAP and heart rate were recorded continuously *via* the arterial catheter in the conscious state over a 3-h period (2 to 5 PM). Continuous recording was performed from 1 to 3 days and again at 4 weeks after SAD operation. Data were sampled every 20 s with an analog-to-digital converter and stored on a Macintosh computer. The average value and standard deviation of MAP were calculated. The standard deviation of MAP was used as an index of blood pressure lability.

Vascular Reactivity of Aortic Rings

Four weeks after SAD or sham operation, the vasoreactivity of isolated aortic rings was evaluated as described previously (*12*, *13*) with slight modification (Fig. 1A). The rats were killed with a lethal dose of anesthetic, and the thoracic aorta was removed. The aorta was dissected free of adherent fat and connective tissue and cut into rings (3 mm in length). The aortic ring was placed horizontally between L-shaped stainless wires in an organ bath chamber filled with oxygenated (95% O_2, 5% CO_2) balanced salt solution (37 °C, pH 7.4) of the following composition: NaCl 112 mmol/l, KCl 4.7 mmol/l, $CaCl_2$ 0.9 mmol/l, $MgCl_2$ 1.2 mmol/l, $NaHCO_3$ 25 mmol/l, KH_2PO_4 1.2 mmol/l, glucose 11 mmol/l, and EDTA 0.026 mmol/l. The aortic ring was connected to a force transducer for isometric tension recording. After a 60-min equilibration period, the ring was gradually stretched to an optimal resting tension of 2 g. Then the ring was contracted by addition of KCl (60 mmol/l) and washed with fresh balanced salt solution. The aortic ring was allowed to equilibrate for 30 min before the experiment.

To test the vasorelaxing reactivity, the aortic ring was precontracted with norepinephrine (100 nmol/l) and then relaxed by cumulative addition of an endothelium-dependent vasodilator, acetylcholine (1 nmol/l to 10 μmol/l), or an endothelium-independent vasodilator, sodium nitroprusside (1 nmol/l to 10 μmol/l). Relaxation was expressed as a percentage of the tension induced by norepinephrine.

NO Production by Aortic Rings

Four weeks after SAD or sham operation, the isolated aortic ring was opened longitudinally and incubated in 1 ml balanced salt solution containing acetylcholine (1 μmol/l) and L-arginine (100 μmol/l) at 37 °C. After 20 or 60 min of incubation, a sample of the solution was collected to analyze ni-

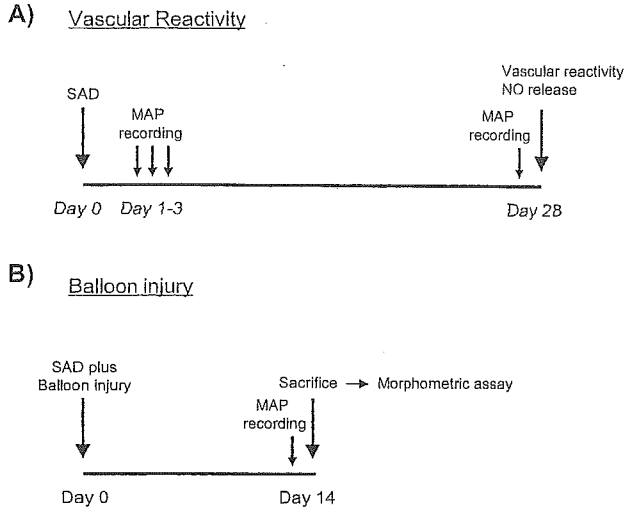

Fig. 1. *Experimental protocols for the vascular reactivity (A) and balloon injury (B). SAD, sinoaortic denervation; MAP, mean arterial pressure.*

trite/nitrate concentration as a measure of NO release. After incubation, the wet weight of the aortic ring was measured. Nitrite/nitrate concentration in the solution was determined using an automatic analyzer that employs automated flow injection analysis (TCI-NOX5000S; Tokyo Kasei Kogyo, Tokyo, Japan) as described previously (*14*). Briefly, the sample (0.1 ml) was diluted with 0.4 ml distilled water, and 0.3 ml 0.3 eq/l NaOH was added. After incubation for 5 min at room temperature, 0.3 ml 5% (w/v) $ZnSO_4$ was added, and the sample was incubated for an additional 5 min. The mixture was centrifuged at 2,800×*g* for 10 min and the supernatant was applied to the analyzer. The nitrite reacted with Griess reagent to form a purple azo compound. The absorbance at 540 nm was measured. The nitrate concentration was determined by means of reduction to nitrite through a copperized cadmium reduction column.

Balloon Injury in the Carotid Artery

In a separate experiment, balloon injury of the carotid artery and SAD (or sham operation) were performed simultaneously in order to investigate the effects of blood pressure lability on neointimal formation (Fig. 1B). Balloon injury was performed as described previously (*15*). Briefly, a 2 French Fogarty arterial embolectomy balloon catheter (Baxter, Irvine, USA) was inserted into the left common carotid artery through the left external carotid artery and advanced to the aortic arch. The balloon was inflated with saline and gradually withdrawn to the carotid bifurcation. This procedure was repeated three times, and then the balloon catheter was removed and the left external carotid artery was ligated.

The rats were killed with a lethal dose of anesthetic 14 days after balloon injury. The carotid artery was perfused and fixed with 4% paraformaldehyde at 100 mmHg and then removed for histological examination.

Morphometric Assay

Morphometric assay was performed as described previously (*16*). The middle third of the fixed carotid artery was embedded in paraffin, and multiple 5-μm cross sections were stained with hematoxylin and eosin or elastica van Gieson. After the section was photographed, the image was scanned and analyzed using NIH Image software. Then, the area of the neointima and of the media and the neointimal-to-medial area ratio were calculated. Three portions of each sample were analyzed, and the mean values were subjected to statistical analysis.

In Vivo Cell Proliferation Assay

Immunohistochemical staining of sections was carried out by the streptavidin-biotin-peroxidase method as described previously (*17*). We used anti-proliferating cell nuclear antigen (PCNA) antibody (PC10, 10 μg/ml; Boehringer Mannheim Biochemica, Mannheim, Germany) and normal mouse IgG (10 μg/ml) as the primary antibody. Specifically bound antibody was visualized by immersing the section in a substrate solution of 3,3-diaminobenzine (Vector Laboratories, Burlingame, USA). The number of positively stained nuclei within the neointima was counted, and the ratio of the number of positive cells to the total number of cells, expressed as a percentage, was calculated as an index of proliferation. Three vision fields of each sample were analyzed, and the mean values were subjected to statistical analysis.

Data Analysis

All values were expressed as the mean±SEM. In the vascular reactivity experiment, the concentration of substance (expressed as −log mol/l) evoking 50% relaxation (pD_2) and the maximum relaxation response (expressed as a percentage of precontraction response) were calculated. Unpaired Student's *t*-test was used for statistical analysis of differences between the two groups. Values of $p<0.05$ were considered to indicate statistical significance.

Results

Baroreflex sensitivity was assessed 3 days after SAD in terms of the reflex reduction in heart rate occurring in response to phenylephrine-induced increase in MAP level. When expressed as the ratio of heart rate decrease to MAP increase, the reflex response in SAD rats ($n=10$) was significantly diminished compared with that in sham-operated rats ($n=6$) (-1.09 ± 0.23 *vs.* -4.43 ± 0.96 bpm/mmHg, respectively, $p<0.01$).

The typical heart rate and MAP recordings of a SAD rat and a sham-operated rat on day 3 are shown in Fig. 2. A

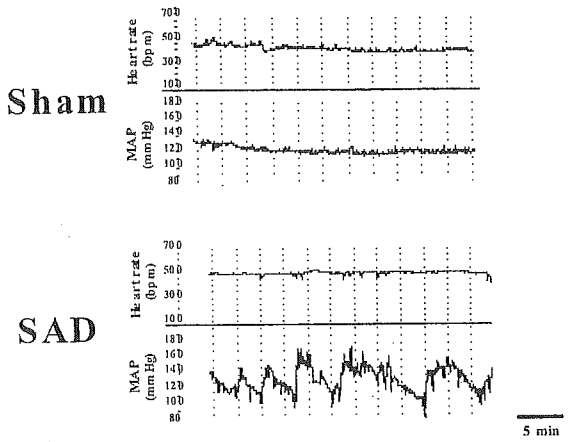

Fig. 2. *Representative heart rate and mean arterial pressure (MAP) recordings of a sinoaortic-denervated rat (SAD) and a sham-operated rat (Sham).*

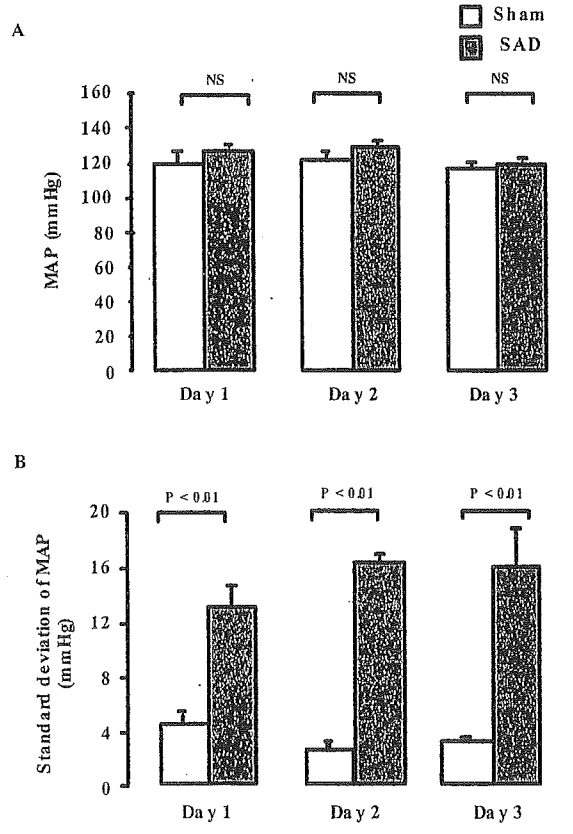

Fig. 3. *Average level of mean arterial pressure (MAP) (A) and standard deviation of MAP (B) from day 1 to day 3 after sinoaortic-denervation (SAD) or sham operation (Sham) in rats. Each bar represents the mean±SEM* (n=*5 for each group).*

marked increase in short-term MAP variability with an equivalent average level of MAP was observed in the SAD rat. A summary of MAP data on days 1–3 after operation is shown in Fig. 3. The average MAP level was not significantly different between SAD rats and sham-operated rats from 1 to 3 days after SAD (or sham operation) (Fig. 3A). However, the standard deviation of MAP, an index of blood pressure lability, was significantly greater in SAD rats at these time points (Fig. 3B). Table 1 shows the effects of SAD for 4 weeks on body weight, heart rate, and MAP. The body weight, heart rate, and average MAP value in sham-operated rats were identical to those in SAD rats. In contrast, the standard deviation of MAP in SAD rats remained significantly greater than that in sham-operated rats. Similar results on average MAP and standard deviation of MAP were obtained at 2 weeks after the operation (data not shown).

Four weeks after SAD or sham operation, the vasoreactivity of isolated aortic rings was evaluated. Maximum contraction in response to norepinephrine (100 nmol/l) was similar in the two groups (Table 2). Endothelium-dependent relaxation in response to acetylcholine was impaired in the SAD group (Fig. 4A). Table 2 shows that both maximum relaxation and sensitivity (pD_2) in response to acetylcholine were

Table 1. Effects of Sinoaortic Denervation for 4 Weeks on Body Weight, Heart Rate and Mean Arterial Pressure in Conscious Rats

	Sham	SAD
Body wegiht (g)	440±12	400±12
Heart rate (bpm)	447±28	486±21
Mean arterial pressure (mmHg)		
Average	121±5.3	124±4.0
Standard deviation	4.7±0.9	13.3±0.9*

Values are expressed as mean±SEM of 5–7 animals. Sham, sham-operated rats; SAD, sinoaortic-denervated rats. * $p<0.01$ *vs.* sham-operated rats.

Table 2. Maximum Response and Sensitivity (pD_2) to Acetylcholine and Sodium Nitroprusside in Isolated Aortic Rings of SAD and Sham

	Sham	SAD
Maximum contraction to norepinephrine (g)	0.84±0.15	0.87±0.05
Acetylcholine		
Maximum relaxation (% of precontraction)	90.6±3.0	66.6±2.2*
pD_2 (−log mol/l)	7.21±0.26	6.44±0.16*
Sodium nitroprusside		
Maximum relaxation (% of precontraction)	98.3±1.3	95.8±1.6
pD_2 (−log mol/l)	6.94±0.12	6.69±0.10

Values are expressed as mean±SEM of 5–7 animals. Sham, sham-operated rats; SAD, sinoaortic-denervated rats. pD_2, concentration evoking 50% relaxation. * $p<0.05$ *vs.* sham-operated rats.